Exploring the potential of conventional and flash pyrolysis methods for the valorisation of grape seed and chestnut shell biomass from agri-food industry waste

R. Pardo [a], L. Taboada-Ruiz [a], E. Fuente [a], B. Ruiz [a], M. Díaz-Somoano [a], L.F. Calvo [b], S. Paniagua [c,d,*]

[a] *Biocarbon, Circularity and Sustainability Group (BC&S), Instituto de Ciencia y Tecnología del Carbono (INCAR), CSIC, Francisco Pintado Fe, 26, 33011, Oviedo, Spain*
[b] *University of León, Department of Chemistry and Applied Physics, Chemical Engineering Area, IMARENABIO, Avda. Portugal 41, 24071, León, Spain*
[c] *Institute of Sustainable Processes (ISP), University of Valladolid, Dr. Mergelina s/n, Valladolid, 47011, Spain*
[d] *Department of Applied Physics, Faculty of Sciences, University of Valladolid, Paseo Belén 7, Valladolid, 47011, Spain*

ARTICLE INFO

ABSTRACT

Residual biomass is a valuable and growing by-product, but often underutilized. This research aims to investigate the possible strategies for the energetic valorisation of agri-food industry wastes: grape seed and chestnut shell. Pyrolysis thermal process was the selected for this work. Applied to biomass, pyrolysis is a promising method for the simultaneous production of biochar, bio-oil, and gas. Two different pyrolysis processes were conducted: conventional pyrolysis at 750 °C and flash pyrolysis at 750 °C and 850 °C. Flash pyrolysis yielded superior product properties compared to conventional pyrolysis. The gas obtained through flash pyrolysis presented a four-fold higher high heating value due to increased CH_4 and H_2 content. Bio-oil contains over 90% of polycyclic aromatic hydrocarbons, and calorific value reached up to 32 MJ kg^{-1} for grape seed, which is 7% more than bioethanol HHV. Biochar can be used both as fuel or as activated carbon precursor due to its high carbon content (91%). Calorific value of chestnut shell biochar (32.7 MJ kg^{-1}), comparable to mineral coals, increased by 72% with respect to the value of this untreated raw material. This work approved the potential of flash pyrolysis as a method to process biomass wastes in a renewable energy scenario.

1. Introduction

The rapid urbanization driven by population growth and improved quality of life has given rise to profound environmental concerns. Notably, the extensive utilization of fossil fuels, particularly coal, has led to elevated levels of greenhouse gas emissions [1]. Therefore, there is an urgent need to explore sustainable and readily available alternatives for energy production. In this regard, renewable energies assume a crucial role in the process of decarbonization [2].

Among renewable energies, biomass is gaining increasing importance. It is the most abundantly available renewable resource on earth and its estimated global production is around $2 \cdot 10^{11}$ tons [3]. Agricultural biomass residues may represent a key raw material for European bioenergy. In general, the interest of biomass residues lies in its possibilities to open up the prospect for the generation of energy in a sustainable way [4]. In fact, biomass electricity generation is expected to rise from 2% in 2015 to 5% in 2060 [5].

There are several approaches for the valorisation of biomass residues. A possible categorization difference between biochemical and thermochemical processes. Thermochemical processes involve fragmentation of biomass in a short period of time using heat [6] and encompass different techniques such as combustion, gasification and pyrolysis. Pyrolysis, in particular, is carried out in the absence of oxygen leading to the thermochemical decomposition of the organic material [7]. The distributions of the three biomass pyrolysis products (solid, liquid and gas fractions) are mainly affected by the biomass heating rate, the reactor types, gas and residence time in the reactor [8]. There are three types of pyrolytic processes: conventional, fast and flash pyrolysis [9].

Flash pyrolysis involves high heating rate, shorter residence time,

---

high heat transfer rate and speedy cooling of the gas. Although clearly influenced by the heat transfer limitation [10], in flash pyrolysis the heating rate could reach up to 2500 °C·s^{-1}, much higher than fast and conventional pyrolysis [11] allowing good thermochemical conversions to bio-fuels [12] Residence time in fast and flash pyrolysis is usually under 10 min, while conventional takes between 10 and 60 min [13]. Peak temperature varies from 500 °C to 900 °C [11]. Researchers are particularly interested in the flash pyrolysis process. Several current studies have validated the investigation and modelling of the pyrolysis kinetics of industrial biomass wastes [14]. Namely: coconut fibre [15], bamboo residues [16], agri-food waste [17] or forestry wood waste [18].

Particularly, this work focused on two different abundant industrial residues in Spain: grape seed (GS) and chestnut shell (CH). Wineries are an important industrial sector in the EU agri-food industry, accounting for 60% of worldwide production with 156 million hectolitres of wine per year. As a byproduct of this production process, around 10.5 to 13.1 million tons of grape pomace are produced [19]. This residue contains a mixture of grape seed, skin, stalks, and substantial quantities of phenolic compounds. As other species, due to their high lignin content, grape seeds do not have suitable properties for feeding livestock [20]. Seeds are often regarded as a feedstock for energy production due to its high energy content, both for biodiesel production [21] and for valorisation through pyrolysis processes [22]. Jimenez-Cordero et al. [23] studied the effect of flash and conventional pyrolysis of grape seed in the range of 300–1000 °C. Chars obtained from the flash pyrolysis of this biomass exhibited a high specific surface area, making them potential candidates for the preparation of granular carbons molecular sieve or raw materials for activated carbons [23].

Additionally, chestnut shell is also a residue from the agri-food industry. The demand for chestnuts has grown in recent years due to its use in the production of gluten-free products. During the peeling process, a significant number of residues, comprising approximately 10–20% of the chestnut's weight, is generated [24]. Current global chestnut production is estimated to be 2 million metric tons, primarily concentrated in southern European countries and Asia [25]).

Fruit shells have been also an interesting source for obtaining bio-fuels through different valorisation processes. Several examples can be found in the current literature. Rasool et al. [26] evaluated the potential of almond shells for the production of bioenergy through pyrolysis. Rojas et al. [27] assessed the potential of peanut shells as source of carbonaceous materials. Previous studies have evaluated the potential of chestnut shell as bioenergy source adsorbent precursor [25–27].

Therefore, under various experimental settings, this research assessed for the first time and in a novelty work the energy valorisation of both grape seed and chestnut shell wastes by conventional and flash pyrolysis. In order to evaluate their potential use as fuel or material precursors, the bio products obtained (char, oil, and gas) were analysed and characterized.

2. Material and methods

2.1. Raw material sampling, pretreatment and size reduction

Chestnut shell (CH) waste was supplied by an industry located in the north of Spain (El Bierzo-León). CH is a residue generated from the peeling process in the preparation of candied products (chestnut cream, marronglacé, etc.). Due to the heterogeneity of this residue, it underwent a milling process (<3 mm) in order to obtain a homogeneous mixture. Grape seeds (GS) consists of a representative sample of defatted grape seed waste from the wine industry after extraction of the oil by cold pressing. Since GS were provided in powder form, no additional processing was required. In addition, the whole sample was divided by the quartering method with a parallel divisor and equidistant partitions walls to obtain representative sub-samples which quantities were able to manage under laboratory conditions [28].

2.2. Characterization of the samples

2.2.1. Chemical characterization

Determination of carbon (C), hydrogen (H) and nitrogen (N) content was conducted using a LECO CHN-2000 equipment instrument (LECO Corporation, Groveport, Ohio, United States). Sulfur (S) content was quantified on a LECO S-144-DR instrument (LECO Corporation, Groveport, Ohio, United States). The oxygen (O) content was calculated by difference. Moisture and ash content were determined on a TGA 701 LECO (LECO Corporation, Groveport, Ohio, United States). Calorific values of residues were determined in an adiabatic calorimeter IKA C4000 (IKA Werke GmbH & Co, Staufen, Germany). Biochar and bio-oil calorific values were calculated using the data related to the elemental analysis. Thus, Doulong-Petit [29], Eq. (1), and Beckman [30], Eq. (2) equations were employed to estimate HHV of biochars and bio-oils, respectively. HHV of gases were estimated by performing material and energy balances.

$$HHV \ (kcal·kg^{-1}) = 8140 \ C + 34400 \ (H–O/8) + 2220 \ S \qquad \text{Eq. (1)}$$

$$HHV \ (MJ·kg^{-1}) = 0.352 \ C + 0.994 \ H + 0.105 \ (S - O) \qquad \text{Eq. (2)}$$

2.2.2. Thermogravimetric analysis and kinetics

Thermogravimetric analysis was carried out using a TGA-Q5000IR thermobalance (TA Instruments, New Castle, DE, EE. UU.). The instrument was earlier calibrated using a known standard to guarantee the correct functioning of the thermobalance. A small representative sample (20–50 mg) was placed in a platinum crucible and heated under a N$_2$ atmosphere (25 ml min^{-1}). Different heating rates were applied (5, 10, 15, 25 and 50 °C·min^{-1}) until a final temperature of 900 °C was achieved. Through this procedure, samples thermogravimetric profiles (TG) were obtained representing the weight loss with respect to temperature. To identify the different stages, it is advisable to derive these TG profiles (DTG profiles).

Regarding kinetic parameters, the isoconversional methods Friedman, Flynn-Wall-Ozawa (FWO) and Kissinger-Akahira-Sunose (KAS) were compared to determined different kinetic parameters what happens throughout the pyrolysis process. The complete procedure for obtaining these parameters was detailed in Ref. [31]. Following them, apparent activation energy was determined for conversion degree (α) values between 0.1 and 0.9. The pre-exponential factor, A, (in terms of the value of the activation energy) was estimated by the Kissinger's equation [32].

2.3. Pyrolysis process

The methodology was based on previous works of the group related to biomass pyrolysis [33–35]. The oven used is an original design, as well as the set-up, which is detailed in those previous studies. This set-up consisted of a horizontal quartz reactor connected to a N$_2$ flow controller, a pair of cooling condensers for the collection of the condensable fraction, and 5L Tedlar sample bags (Supelco Analytical, USA) for collection of the gaseous fraction. The boundaries of the reactor in contact with the oven were filled with ceramic refractory fibers to reduce heat losses. In addition, a heating tape was used to cover the rear of the reactor (gas outlet) and prevent condensation of liquids in there. This ensured that all bio-oils were condensed in the heat exchanger and that there was no residue left at the end of the reactor or in the pipes connected to the condenser.

To carry out the experiment, 5–8 g of sample were placed in an alumina crucible (Sigma-Aldrich, USA). Two different pyrolysis processes were carried out: conventional pyrolysis (PC) and flash pyrolysis (PF). PC was performed under a N$_2$ flow of 100 ml min^{-1}, a heating rate of 25 °C·min^{-1}, and a final temperature of 750 °C for 1h. Gas and liquid fraction were collected between 200 °C and 600 °C (according to TG

Table 1
Comparison of biomass chemical characterization.

Biomass	Ash[a] (%)	C[a] (%)	H[a] (%)	O[a] (%)	N[a] (%)	S[a] (%)	HHV (MJ·kg^{-1})	Reference
GS	4.1	50.9	5.4	36.9	2.5	0.2	20.5	This study
CH	0.8	50.4	5.3	43.1	0.4	0.0	19.0	This study
Pomegranate peel	3.1	46.5	4.9	45.0	0.4	0.1	17.1	[34]
Grape marc	3.5	43.2	5.9	45.5	0.7	1.2	20.1	[40]
Mango husk	0.58	47.9	6.0	46.0	0.09	0	19.02	[48]
Mango seed	1.10	40.6	3.99	54.1	1.2	0.1	13.42	[48]
Orange seed	3.09	63.31	9.33	24.63	2.54	0.19	n.d.	[51]
Orange husk	1.59	43.32	6.23	49.79	0.47	0.19	n.d.	[51]

*Oxygen content calculated by difference.
n.d. Not determined.
[a] Dry basis.

results). In the PF the sample was introduced instantaneously when the oven reached the target temperature (750 °C and 850 °C) and maintained for 10min with a flow of N_2 of 100 ml min^{-1}. The extraction of the bio-oils from the condenser required to use dichloromethane (CH_2Cl_2) solvent. The solution of CH_2Cl_2 and the bio-oils fraction was passed through a column filled with sodium sulphate anhydrous (Na_2SO_4) and glass wool. Subsequently, the solutions were stored in glass containers, sealed and refrigerated at a temperature of -3 °C (optimal conditions for the subsequent chromatographic analysis).

About the yields, apart from a homogeneous collection and recollection of the samples, a deeper understanding of the secondary reactions is necessary to control the quality of bio-oil or the yield of target products in fast pyrolysis [36]. The yields were calculated according Eq. (3):

$$\eta \ (\%) = \frac{W_1}{W_0} \cdot 100 \qquad \text{Eq. (3)}$$

where η is the yield, W_1 is the bio-char or bio-oil mass and W_0 refers to CH or GS mass. The gas yield is the result of subtracting from 100 the biochar and bio-oil yields.

2.4. SEM-EDX

Biomass and biochar obtained from conventional and flash pyrolysis were examined with FEI Quanta 650 FEG scanning electron microscope (SEM) (FEI Company, United States) equipped with an Energy Dispersive X-ray Spectrometer. Before analysis, it was necessary to metallize the samples with Iridium to ensure the conductivity of the material and obtain an optimal resolution of the images. This procedure was done in an Emitech K575X metallizer.

2.5. Chromatographic analysis

Chromatographic analysis of the gas fraction was performed on an Agilent 7890A gas chromatograph (Agilent Technologies, Wilmington, DE, USA). The system had five valves and three detectors, two TCD (thermal conductivity detector) and one FID (flame ionization detector). The first TCD was configured with helium as a mobile phase for the analysis of permanent gases (CO_2, CO, O_2, N_2, H_2S, among others). The second TCD was configured with N_2 as the mobile phase for hydrogen analysis. The FID detector was configured for the analysis of hydrocarbons of one to five carbons, grouping those greater than six in a single peak.

An Agilent 7890A gas chromatograph coupled to an Agilent 5975C mass spectrometer was used for the analysis of the bio-oil fraction (Agilent Technologies, Wilmington, DE, USA). An HP-5MS capillary column (Agilent Technologies, Wilmington, DE, USA) (5% phenyl-methylpolysiloxane) with 30 m × 0.25 mm ID x 0.25 μm dimensions, was employed to separate the compounds. Above this test, the water present in the bio-oils fraction was separated from the organic fraction. Liquid sample was injected into the chromatograph when the column

Table 2
Biomass compositional analysis (wt.% dry basis).

Biomass	Hemicellulose (%)	Cellulose (%)	Lignin (%)	Extractives (%)	Reference
GS	18.71	15.68	49.23	13.83	[41]
CH	22.64	31.61	42.69	1.86	[41]
Sweet cherry seed	37.96	23.10	32.94	4.69	[42]
Softwood	25–30	35–40	27–30	n.d.	[43]
Hardwood	20–25	45–50	20–25	n.d.	[43]
Wheat straw	20–25	33–40	15–20	n.d.	[43]
Orange peel waste	6.03	43.75	5.25	23.48	[43]
Peach stone	14	46	33	7	[47]

n.d. Not determined.

reached 50 °C. The sample was maintained until it reached 300 °C (with a heating rate of 4 °C·min^{-1}) to ensure proper volatilization of the sample and separation of its components in order to be accurately detected by an FID detector. The mass spectrometer was operated in full scan mode (50–550 uma, 3.21 scans per second, 70 eV ionization voltage). To identify the compounds detected in the spectrometer, the NIST08 and Wiley 7 N libraries were used.

3. Results and discussion

3.1. Raw materials chemical characterization

Grape seed, chestnut shell and other raw materials fuel properties were collected in Table 1. The samples showed significant differences in ash and nitrogen (N) content. Grape seed (GS), with similar results as presented by Ref. [37], displayed higher ash content (4.1%) compared to chestnut shell (CH) (0.8%). Dhyani and Bhaskar [38] showed that ash content ranged from less than 2% in softwoods to as much as 15% in herbaceous biomass and agricultural residues. Similarly, Vassilev et al. [39] estimated an average ash content of 7.2% based on a review of 532 biomass varieties Comparing these findings to the present study, it is evident that the ash content in GS aligns with other lignocellulosic biomass residues. However, the 0.84% ash content obtained in chestnut shell indicated a minimal presence of mineral matter, which could be beneficial for certain applications. About nitrogen (N), GS had higher values than CH, 2.5% vs. 0.4%.

Regarding the other measured parameters (moisture, C, H, S, O, and heating value), no major differences were observed between GS and CH. Both had a high C content (50%), which may be indicative of good energy conversion [11]. Compared with similar lignocellulosic residues (Table 1), differences were also reduced for these parameters (C, H, S, O and heating value). It can be seen that carbon content ranges between
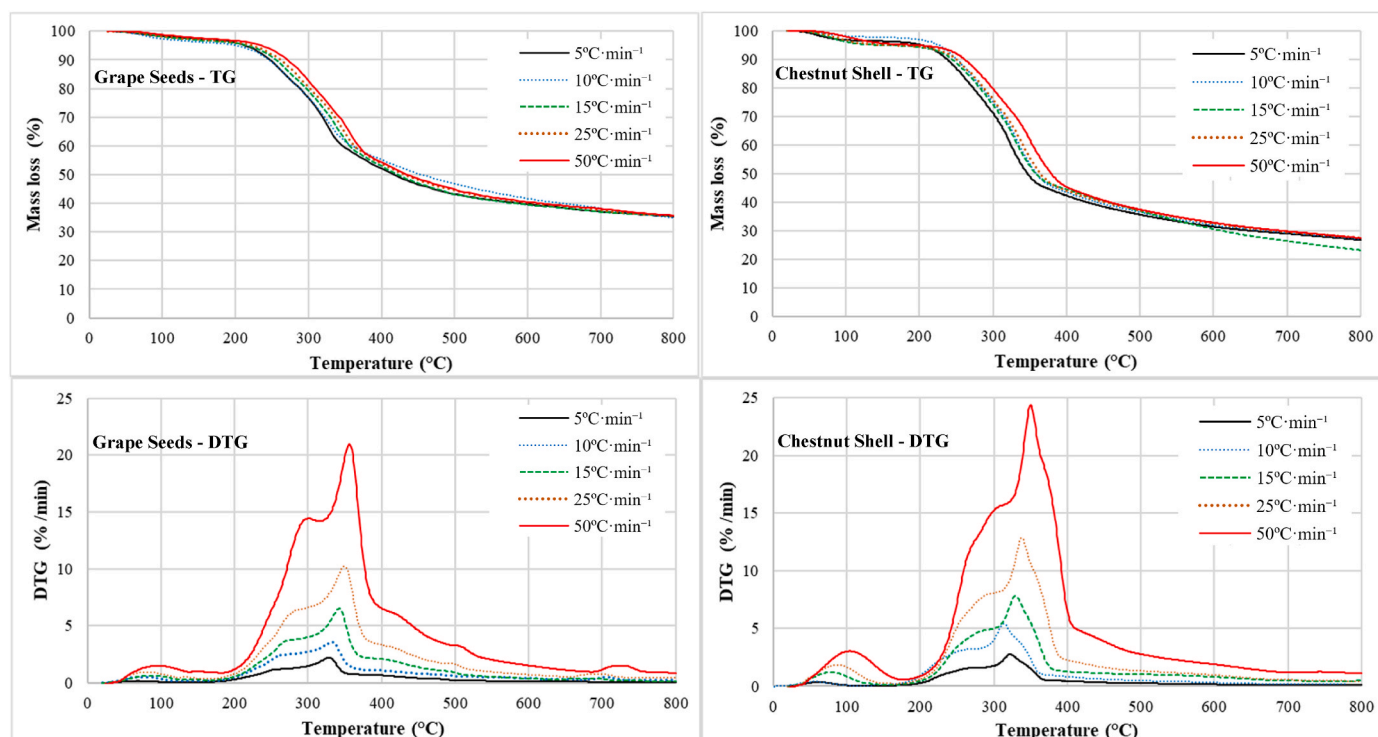
Fig. 1. Grape seeds (GS) and Chestnut shell (CH) DTG and TG pyrolysis profiles for five different heating rates.

40.6 and 63.3% (average of 49.8%); hydrogen varies from 3.99 to 9.33% (average of 5.9%); oxygen goes from 24.6 to 49.8 (with an average of 43%); nitrogen ranges from 0.09 to 2.5% (average of 1%); finally, sulfur varies from 0,0 in CH to 1.2% in grape marc [40]. GS and CH sulfur content was very small (<0.2%), which is advantageous as it helps prevent the formation of sulfur oxides.

About compositional analysis, Table 2, literature [41] referenced grape seeds composition in 18.71% hemicellulose, 15.68% cellulose, 49.23% lignin and 13.83% extractives. Chestnut shell: 22.64% hemicellulose, 31.61% cellulose, 42.69% lignin and 1.86% extractives. Taking special care with the methodology employed for the determination of these parameters (as warned by Ref. [42], specially related to the lignin content), a series of comparison can be made with other energy sources. The lignin content of both samples stands out from the average content shown by lignin in softwood species (27–30%), hardwood species (20–25%) [43]. This higher content leads, as will be discussed in the next paragraph, to higher HHV results, since the energy content of lignin is 30% higher than that of cellulose or of hemicellulose [44]. CH had a so similar hemicellulose and cellulose content to wheat straw. This CH overall sugar content (54.25%) was also higher than orange fruit peel-waste (49.78%) [45]. When compared to others seeds, grape seeds had higher lignin values than cherry seeds [46] or peach stone [47], but lower content of sugars.

Respecting calorific values, HHV ranged between 17 and 20 MJ kg^{-1}, which were similar to those obtained with other lignocellulosic biomass residues [48].

3.2. Thermogravimetric analysis and kinetics

Thermogravimetry (TG) and derivative thermogravimetry (DTG) profiles of CH and GS were shown in Fig. 1. Two stages or peaks of weight loss were identified according to the decomposition of the different components. The first one (~100 °C) was associated with the evaporation of the water presented in the sample, whereas the second one, the most representative, was linked to the release of hemicellulose, cellulose and lignin (200–450 °C) [49]. Most of the sample was

decomposed at this second peak. Due to the polymeric composition of lignocellulosic materials, the interaction is complex coexisting at least two mechanisms during the pyrolysis process. Thus, CH and GS profiles denoted an overlapping. This could be explained by comparing this work results with another undertaken for similar biomass sources, sugarcane bagasse [50] or mango seeds [48] and carried out under similar pyrolysis. All these authors suggested that, as it happened with CH and GS, the first stage of the degradation can be attributed to the decomposition of hemicellulose (200–300 °C) and the second peak is due to the cellulose release (350–370 °C). In the same way, the thermal episode corresponding to the degradation of lignin would be completely overlapped by those two peaks [51]. Hence, and known the similar lignin content of the samples, the slightly higher DTG values for chestnut compared to grapes may be due to its higher sugar (hemicellulose and cellulose) content.

The heating rate also influenced, although not greatly, the tests. It was observed how the lowest ramp (5 °C·min^{-1}) was under which the mass release for the second peak occurred at a lower temperature and with the lower values. Note how for both biomass sources, the highest DTG point was achieved under the 50 °C·min^{-1} heating rate. CH DTG$_{max}$ values were slightly higher than their homonymous for GS. CH maximum for this parameter was 24.36%·min^{-1} vs. the 20.97%·min^{-1} reached by GS. The final solid residue presented in TG profiles (% by weight) was very similar. In the case of GS, they varied between 33%-34% and 24%–27% for CH. Moreover, the results obtained were in line with thermogravimetric analyses for similar biomass sources [52].

In general, both biomass wastes studied by thermogravimetry showed very similar results. The stability of the final weight loss allows us to decide the working temperatures for both types of pyrolysis 750 °C and 850 °C, as well as the optimum moment of gas collection in the PC between 200 and 600 °C.

With an optimal fitting (R^2 values close to 1 for almost all cases), Fig. 2, kinetic results (Table 3) denoted higher E$_a$ and A results for GS regardless of the model employed. E$_a$ values rated 212.35–217.19 kJ mol^{-1} for CH and 336.83–349.13 kJ mol^{-1} for GS. Considering conversion degree, for GS, there was a trend characterized by an increase in
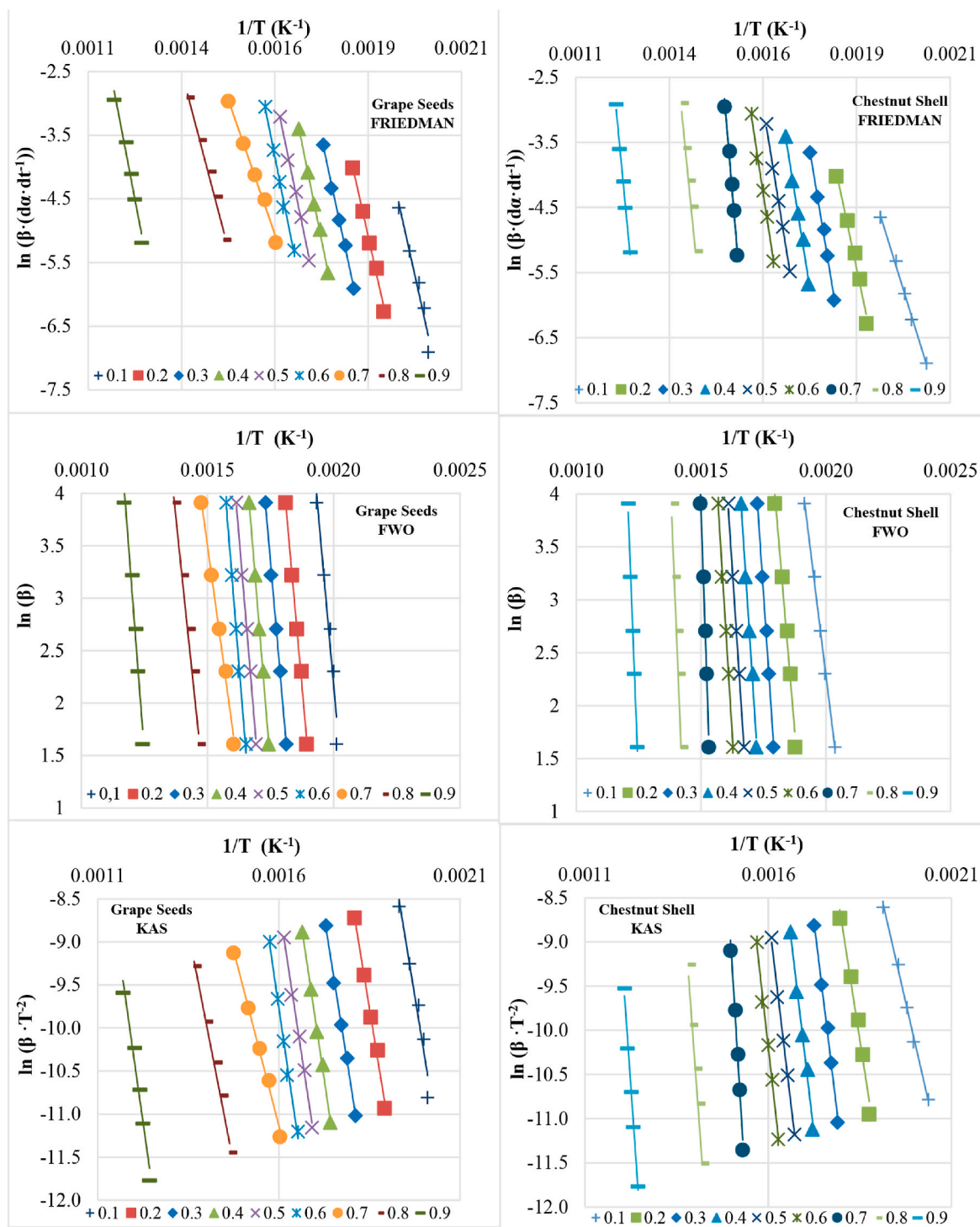
Fig. 2. Linear plot for Friedman, FWO and KAS for CH (left column) and GS (right column).

activation energy as the degree of conversion also increased. The minimum E_a values were obtained for this biomass sample under 0.1 conversion degree. However, this behaviour was not observed for CH. 0.7 conversion degree was the one linked to CH E_a minimum values. E_a variations were attributed to changes in the decomposition mechanism given the proportions of reactive compounds as well as the occurrence of possible secondary reactions such as cooking/charring [53]. Values here obtained for CH were in line with other biomass waste like mustard stalk [54] while GS kinetic results were closer to the different parts of similar seeds already studied [55].

3.3. Pyrolysis process

3.3.1. Yield

A notable variation was observed between the results of conventional and flash pyrolysis, Fig. 3. The secondary reactions together with the differences in the nature composition of the samples may be the cause of these variations. In the case of GS conventional pyrolysis, the principal fraction was bio-oil (40.33%), although similar to biochar (37.59%) and much higher than the gaseous fraction, which represented only 22.09%. However, in the experiments with flash pyrolysis, the

Table 3
Kinetic parameters.

Sample	α	FRIEDMAN			FWO			KAS		
		E_a (KJ mol^{-1})	R^2	A (s^{-1})	E_a (KJ mol^{-1})	R^2	A (s^{-1})	E_a (KJmol^{-1})	R^2	A (s^{-1})
CH	0.1	219.00	0.9562	6.9E+22	212.19	0.9578	1.33E+22	214.78	0.9545	2.5E+22
	0.2	216.55	0.9944	1.3E+21	212.97	0.9947	5.56E+20	215.06	0.9942	1.2E+21
	0.3	217.30	0.9954	1.6E+20	211.00	0.9956	4.10E+19	212.64	0.9952	5.9E+19
	0.4	241.15	0.9981	3.9E+21	233.87	0.9982	8.40E+20	236.27	0.9980	1.4E+21
	0.5	235.42	0.9929	2.3E+20	228.56	0.9932	6.53E+19	230.39	0.9926	9.5E+19
	0.6	245.13	0.9902	5.3E+20	237.91	0.9906	1.26E+20	239.98	0.9898	1.9E+20
	0.7	140.88	0.9938	1.4E+11	139.05	0.9943	9.98E+10	135.48	0.9932	5.0E+10
	0.8	185.09	0.9917	3.7E+13	181.54	0.9922	1.97E+13	179.22	0.9911	1.3E+13
	0.9	254.20	0.9689	8.5E+15	248.20	0.9706	3.47E+15	247.30	0.9671	3.0E+15
	a	**217.19**		**8.4E+21**	**211.70**		**1.7E+21**	**212.35**		**3.1E+21**
GS	0.1	154.37	0.9963	9.8E+15	150.74	0.9965	4.0E+15	150.16	0.9961	3.5E+15
	0.2	228.30	0.9827	1.3E+22	221.32	0.9833	2.7E+21	223.77	0.9819	1.1E+22
	0.3	302.16	0.9900	1.0E+28	291.69	0.9903	1.1E+27	297.45	0.9896	3.7E+27
	0.4	298.70	0.9903	4.1E+26	288.60	0.9906	5.0E+25	293.78	0.9899	1.5E+26
	0.5	293.82	0.9960	1.8E+25	284.11	0.9962	3.1E+24	288.75	0.9959	8.0E+24
	0.6	313.50	0.9905	2.2E+26	302.96	0.9908	2.9E+25	308.30	0.9902	8.1E+25
	0.7	566.37	0.9826	1.7E+45	543.60	0.9829	2.6E+43	560.88	0.9822	6.2E+44
	0.8	482.73	0.9837	3.6E+35	464.51	0.9841	1.6E+34	476.79	0.9833	1.3E+35
	0.9	502.21	0.9902	2.0E+32	483.83	0.9904	1.3E+31	495.42	0.9899	7.2E+31
	a	**349.13**		**1.9E+44**	**336.82**		**2.8E+42**	**343.92**		**6.8E+43**

[a] mean values.
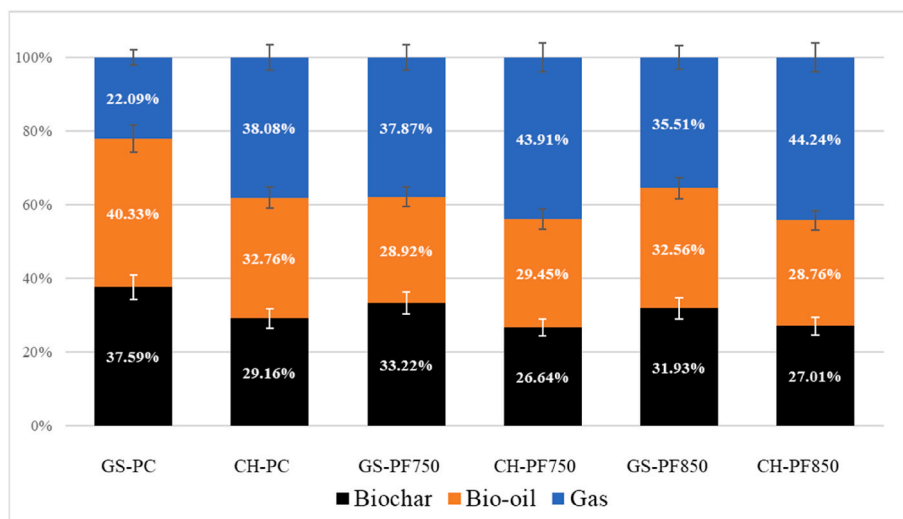
Fig. 3. Yield of gas, bio-oil and biochar fractions in the different pyrolytic processes.

gaseous fraction was the majority, with 37.87% at 750 °C and 35.51% at 850 °C. It could also be seen that PF decreased the formation of bio-oil in favour of gases, going from 40.33% of bio-oil in PC, to 28.92% and 32.56% at 750 °C and 850 °C respectively. These results were in concordance with the previously obtained, since flash processes at high temperature seem to be related to higher gas formation, as could also be seen in previous experiments with pampa grass and pomegranate peel [33,34]. Slower heating rate in conventional pyrolysis minimized the thermal cracking reactions taking place within the biomass, resulting in higher yields of char. On the other hand, higher heating rates in flash pyrolysis promoted the thermal fragmentation and cracking reactions taking place which hinders the formation of chars, and thus increasing the liquid and gas yields [56]. Although it is common to find in the literature higher bio-oil yields linked to flash pyrolysis, it is important to note that these results are highly dependent on the type of biomass [11]. In addition, Tsekos C. et al. [57] working with woody biomass, found that liquid production peaks at round 600 °C, and decrease from 600 °C to 800 °C.

Results were consistent with those obtained in DTG solid residue for grape seed, where a char yield of over 34% was obtained. These GS char values were higher than expected when compared to another biomass pyrolysis. Working in the 750–850 °C range, char yields usually vary around 20–30% [58], while in this work they reached 37.59% in conventional pyrolysis. Alper et al. [59], obtained a 29.82% yield at 800 °C in the pyrolysis of grape seed.

Regarding the chestnut shell waste, the yield fraction quantitative differences between conventional pyrolysis and flash pyrolysis were smaller than in grape seeds case. For conventional pyrolysis, the gas fraction represented 38.08%, while in flash pyrolysis it increased to 43.91% and 44.24% at 750 °C and 850 °C respectively. The change observed in the amount of bio-oil was similar. It varied from 32.76% in the conventional pyrolysis, to 29% in the flash pyrolysis. About the char yield, it decreased from 29.16% in PC to values around 27% in both PF; being the results consistent with those obtained for CH by thermogravimetry (up to 27%). In a previous study of chestnut shell pyrolysis carried out by Ruiz et al. [60], a slightly higher average yield was obtained for char (34.14%). However, this waste had a higher composition of ashes than CH of this work (2.11% *vs.* 0.8%), which contributed to a
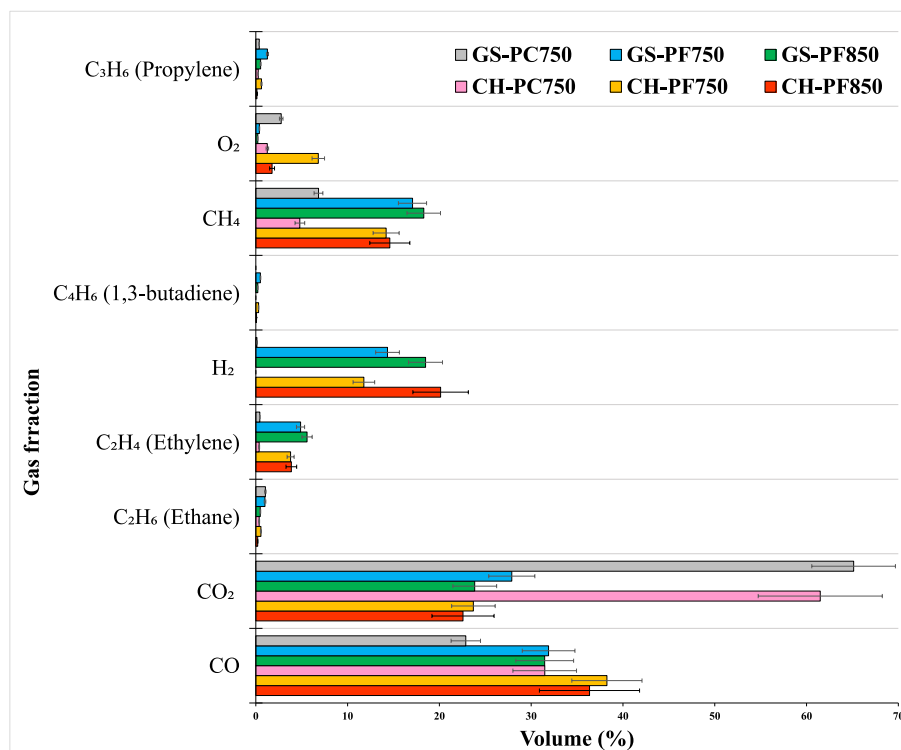
Fig. 4. Composition of the gas fraction for the different samples and pyrolysis processes.

higher char yield, since the ashes were concentrated in the solid fraction of the pyrolysis process (char ash content: 4.78% in Ruiz et al. [60], *vs.* 2.39% in this work).

3.3.2. Gas fraction

Chromatographic analysis of the gases (Fig. 4) showed a clear difference between the two types of pyrolysis (PC and PF). The main gases were CO_2, CO, CH_4 and H_2. According to Kan et al. [61], CO_2 and CO were mainly produced from the decomposition and reforming of carbonyl (C═O) and carboxyl (COO) groups. Light hydrocarbons such as CH_4 came from the decomposition of weakly bonded methoxyl (-O-CH_3) and methylene (-CH_2-) groups, as well as secondary decomposition of oxygenated compounds. H_2 can be obtained as a result of the decomposition and reforming of C═C and C–H aromatic groups at high temperatures [61].

In PC, CO_2 production was much higher, exceeding 60% in both materials, while in flash pyrolysis it was reduced to less than 25% in all cases. CO was also influenced by the type of pyrolysis, although to a lesser extent, going from 22% (in PC) to 32% (in PF) with the grape seed waste, and from 31% (in PC) to 38% (in PF) in the case of chestnut shell waste. This was relevant, since a similar effect has been detected in gases with biofuel potential (CH_4 and H_2) [62]. In the case of CH_4, the amount produced in the flash pyrolysis tripled with respect to the conventional pyrolysis, going from 6.83% to 17.17% and 18.46% at 750 °C and 850 °C respectively for GS. Chestnut shell gas changed from 4.79% to 14.2% and 14.6%. The case of H_2 was even more significant, since 0.12% H_2 was detected in grape seed in conventional pyrolysis, while it reached 14.43% in PF750 and 18.65% in PF850. Likewise, the conventional pyrolysis gas from CH waste does not contain H_2 but reached 11.77% in PF750 and 20.13% in PF850. Given the growing interest in both gases (CH_4 and H_2) for their potential use as biofuels, this was highly relevant.

Comparing these results with those obtained by Refs. [33,34], it can be seen that both biomasses had a very similar behaviour in general terms. CO_2 and CO are the most abundant gases, while CH_4 and H_2 content increased notably in the flash processes. However, some differences were observed in the amounts of CH_4 and H_2 obtained. For

Table 4
Bio-oil and Bio-char analysis.

Bio-oil						
Sample	Ash[a] (%)	C[a] (%)	H[a] (%)	N[a] (%)	S[a] (%)	O[a] (%) *	HHV (MJ·kg^{-1})
GS-PC750	n.d	64.36	7.31	5.69	n.d.	22.64	27.54
GS-PF750	n.d	74.28	5.95	6.57	n.d.	13.21	30.67
GS-PF850	n.d	78.64	5.57	4.78	n.d.	11.01	32.06
CH-PC750	n.d	53.31	6.19	1.34	n.d.	39.17	20.80
CH-PF750	n.d	67.94	6.19	4.47	n.d.	21.40	27.83
CH-PF850	n.d	77.03	5.90	2.11	n.d.	14.96	31.41
Bio-Char						
GS-PC750	8.72	80.14	1.31	1.99	0.05	7.79	27.78
GS-PF750	10.23	77.60	1.60	1.91	0.07	8.59	27.19
GS-PF850	9.70	77.45	1.32	1.86	0.08	9.59	26.56
CH-PC750	2.39	91.38	1.22	1.07	0.01	3.93	32.17
CH-PF750	3.59	90.32	1.77	0.97	0.00	3.35	32.71
CH-PF850	2.83	91.54	1.20	1.06	0.04	3.33	32.31

n.d. Not determined.
*Oxygen content calculated by difference.
[a] Dry basis.

pampa grass, the maximum percentage of methane was around 8%, and 12% for pomegranate peel. In our case methane reached 18.5% and 14.6% for grape seed and chestnut shell. For H_2 [33], obtained 16%, while [34] reached 19%. In our case, we obtained 18.65% with GS and 20.1% with the CH.

Gas HHV results obtained from grape seed pyrolysis were 4.33 MJ kg^{-1}, 15.35 MJ·kg^{-1} and 16.64 MJ kg^{-1} (for PC at 750°, PF at 750° and PF at 850 °C respectively). With chestnut shell HHV resulted slightly lower than GS: 3.96 MJ kg^{-1}, 12.92 MJ·kg^{-1} and 14.74 MJ kg^{-1} (for PC
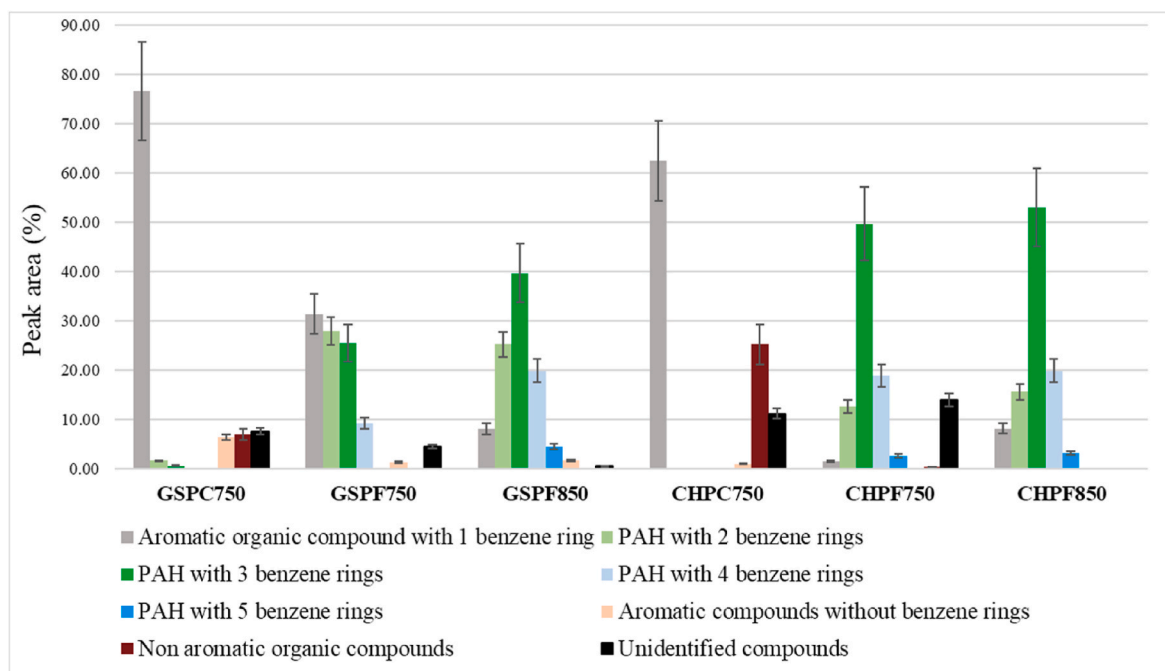
Fig. 5. Chromatographic analysis of bio-oil.

at 750°, PF at 750° and PF at 850 °C respectively). It was observed that in both cases the HHV almost quadrupled in the flash pyrolysis processes compared to conventional pyrolysis, going from 4.3 MJ kg^{-1} to 16.6 MJ·kg^{-1}in the case of grape seed, and from 3.96 MJ kg^{-1} to 14.7 MJ kg^{-1} with chestnut shell. This large variation was mainly due to the increase in the amount of H$_2$ and CH$_4$ produced in flash pyrolysis, as already seen in Ref. [63]. Compared to these studies, the highest HHV of gases obtained with pampa grass biomass was 17.2 MJ kg^{-1} [33] and 11.5 MJ kg^{-1} with pomegranate peel [34].

Flash pyrolysis gases had a higher calorific value because their composition had a lower CO$_2$ content and a higher content of fuel gases (H$_2$, CH$_4$, C$_2$H$_4$). Also, gas obtained through pyrolysis flash at 850 °C showed higher calorific value than at 750 °C. According to Ighalo J. et al. [11], the increase in H$_2$ formation can be attributed to the rearrangement and condensation of aromatic rings and dehydrogenation of char as temperature increases.

3.3.3. Bio-oil

In order to determine the bio-oils elemental composition, Table 4 was elaborated. The pyrolysis type clearly influences the nature. For both materials, a notable increase in carbon content was observed in the flash pyrolysis with respect to the conventional pyrolysis, similar to Pérez et al. [33] with pampa grass biomass. In our study, at PF850, the amount of C achieved were similar for both biomass: up to 77.03% and 78.64% of C content for chestnut shell and grape seed bio-oils, respectively. Employing similar experimental conditions [33], achieved up to 86,7% with pampa grass biomass. Compared with other studies [38], review threw an average of 47% of carbon content for twenty-seven different bio-oil samples (carried out in different conditions). Bio-oil obtained from chestnut shell and grape seed was comparable to diesel in terms of carbon content (81.4%) [64]. The maximum nitrogen levels were obtained in flash pyrolysis at 750 °C for both residues. Also [33], obtained higher N concentrations in PF at 750 °C (5.32% of N), although with a slightly higher percentage in our case (6.57%). These N concentrations were higher when compared with other biomass [38] which could limit its potential as a biofuel due to the possible release of nitrogen oxides. However, there are technologies available that can mitigate these problems, such as fuel optimization and pre-combustion control or the use of exhaust gas recirculation (EGR) technologies,

among others [65].

Regarding the calorific value of the bio-oils, as happened for gas fractions, there was an increment in the HHV as the pyrolysis temperature increased. This raise was especially noticeable in the case of chestnut shell bio-oil, where it was from 20.8 MJ kg^{-1} at PC750 to 31.4 MJ kg^{-1} at PF850. In both cases these HHV values were higher than most of the bio-oils studied in the review of Dhyani and Bhaskar [38]. In the case of GS, the increase was not as significant than in CH, but it reached up to 32 MJ kg^{-1}, higher than bioethanol (29.7 MJ kg^{-1}) and not so far from biodiesel (37.7 MJ kg^{-1}) [66].

Bio-oil samples were also analysed by GC-MS, detecting between 40 and 50 different organic compounds in each of them. Based on the study of Pérez et al. [33], compounds were classified according to aromaticity and the number of benzene rings of each compound, as shown in Fig. 5. The full liquid chromatograms, liquid analysis (GCMS) and identification of the peaks were presented in the Supplementary Material file.

In the case of conventional pyrolysis, single-ring aromatic hydrocarbons predominated (70–80%), such as benzene and some derivatives, mainly phenols. The presence of polycyclic aromatic hydrocarbons (PAH) was very low (<3% in both cases). Aromatic compounds without benzene rings were also detected (some of them were nitrogenous pyridine derivatives; 6% in the case of grape seed and 1% in chestnut shell). Finally, non-aromatic compounds, mostly aliphatic hydrocarbons, were found representing 10% and 28% in grape seed and chestnut shell, respectively.

The results obtained by flash pyrolysis were very different compared to conventional pyrolysis. In the flash processes (PF750 and PF850), for both samples, PAHs (naphthalenes (2 rings), anthracenes (3 rings), phenanthrenes (3 rings), pyrenes (4 rings) or fluoranthenes (5 rings)) were predominant. Nonetheless, the presence of single ring aromatic compounds, non-aromatic compounds and aliphatic hydrocarbons was reduced. PAHs accounted for 65%–90% of the total compounds detected in the flash pyrolysis.

In general, the results were similar to those obtained in the pyrolysis of other residues such as agro-indrustrial biomass [67], palm kernel shell [63] or pampa grass [33]. In these studies, PAHs with between 2 and 5 benzene rings were the most abundant compounds in flash pyrolysis processes, whereas in conventional pyrolysis the predominant elements were simple aromatic compounds with one benzene ring.
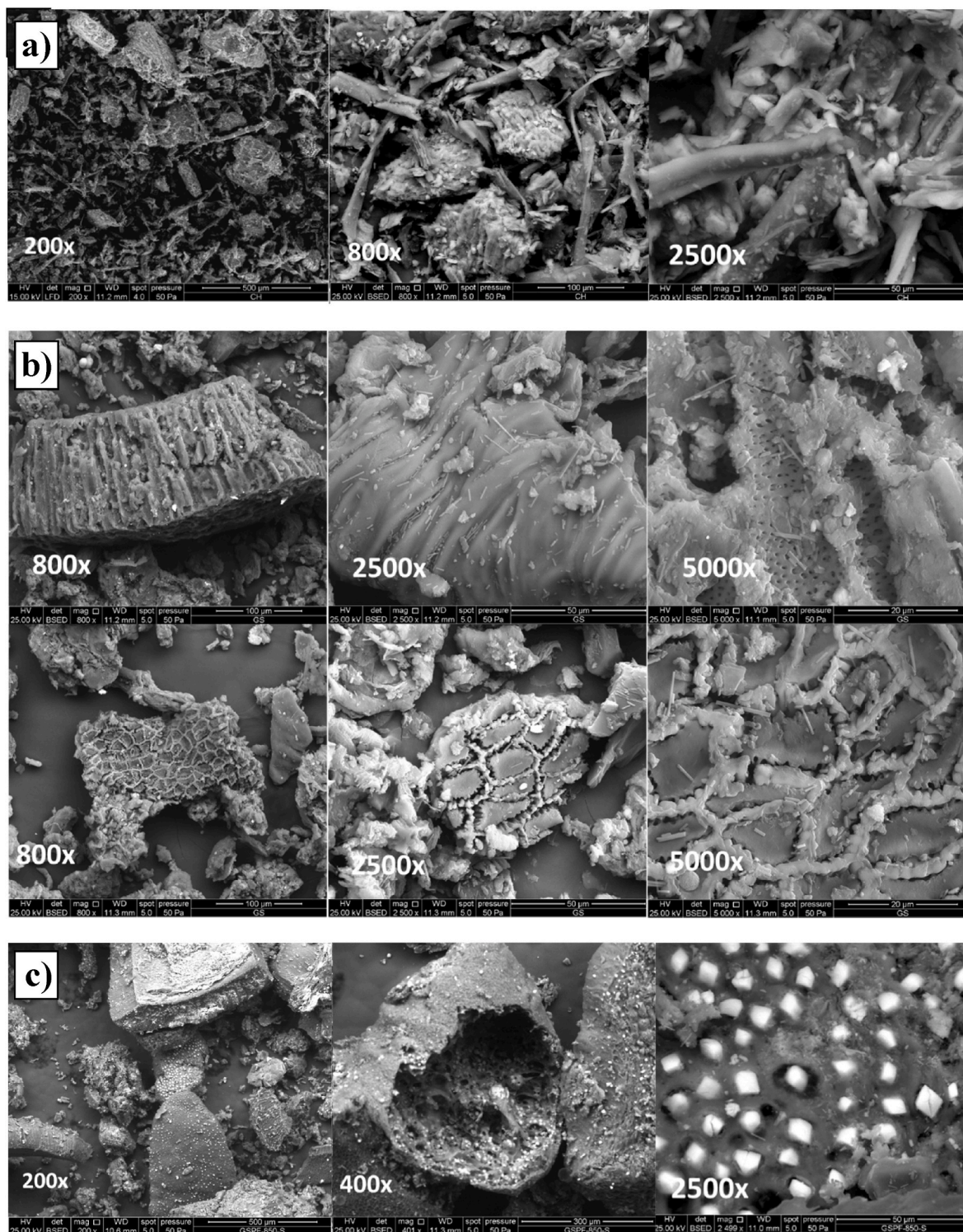
Fig. 6. SEM images detail for CH and GS materials at different magnifications: a) Fibrous and laminar parts of CHPC750–S. b) Tubular structures of GSPC750-S that probably correspond to seed tegument. c) Hollows in GSPF850-S probably caused by the rapid heating in flash pyrolysis.

The difference in bio-oil composition between conventional pyrolysis and flash pyrolysis could be attributed, among others, to the shorter residence time in flash pyrolysis of 10 min compared to 60 min in conventional pyrolysis. Longer residence times of volatiles in the reactor may result in secondary reactions causing the breakdown of primary volatiles [68]. Also, Tsekos et al. [57] found a relationship between PAH temperature and abundance. At intermediately high temperatures, secondary reactions took place in the gas phase converting the

oxygen-containing tar compounds produced primarily to light hydrocarbons, aromatics, oxygenates and olefins. As result of this, higher hydrocarbons and larger polycyclic aromatic hydrocarbons can be formed.

Overall, it could be stated that both temperature and residence time have great influence on the composition of the bio-oil. It is also important to mention that, given the abundance of nitrogenous compounds in bio-oils, their application as biofuels would not be optimal, although
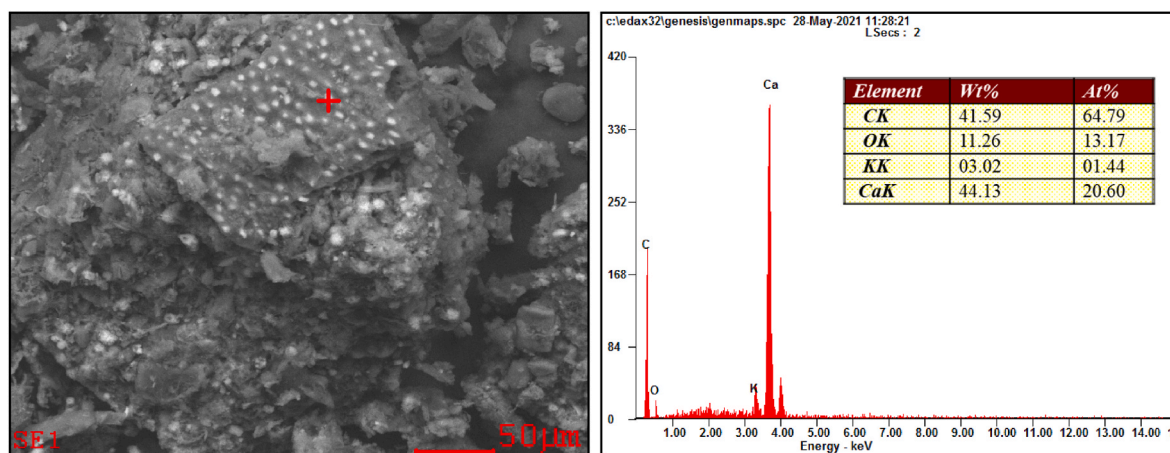
Fig. 7. SEM-EDX detail for GS.

they could be used for the synthesis of organic compounds [69]. For example, some compounds derived from the degradation of cellulose and hemicellulose, such as furan and its derivatives, are used as solvents for resins and for the synthesis of chemical products such as insecticides, stabilizers and pharmaceutical products [34]. Additionally, the breakdown of lignin produces benzenes and phenolic compounds, which possess applications in the creation of synthetic resins, dyes, pesticides, solvents, and lubricants [34,58].

3.3.4. Biochar

Table 4 shows the elemental composition and calorific value of the different biochar obtained by pyrolysis. C content ranged between 77 and 80% for grape seeds and 90–91% for chestnut shells. The highest content in this element was linked to CH-PF850, 91.54%. Other published works related to pomegranate peel and pampa grass pyrolysis rated up to 83% and 85% contents respectively [33,34].

Compared to mineral coals, the material obtained from CH was close to coals with high degree of metamorphism. A higher C content in the biochar will result in a higher calorific value [11] and, given its chemical characteristics, will also allow its use as a precursor of carbonaceous materials with good adsorption properties.

Biochar obtained from CH had a calorific value of about 32 MJ kg^{-1}, while GS had a calorific value around 27 MJ kg^{-1}. Compared with the original biomass, GS increased the HHV by more than 35% (from 20.5 to 27.78 MJ kg^{-1}) and CH raised by over 72% (from 19 to 32.71 MJ kg^{-1}). Both results were on line or higher than wood residue biochar [70] or other common waste like coffee grounds [71] or palm kernel shells [72].

Therefore, the biochar obtained from chestnut shells and grape seed would be good candidates for different applications (including like adsorbent materials [73]).

3.4. SEM-EDX

The morphological analysis of GS and CH biomass was performed by SEM-EDX (Figs. 6 and 7). In both cases vegetal structures of plants have been preserved after the pyrolysis process. Some differences between residues (GS and CH) can be appreciated. In the CH residue two different parts can be observed: one of them with fibrous structure, and other laminar, similar to the original residue (Fig. 6a). Regarding GS, tubular structures were found associated to the seed tegument (Fig. 6b), formed by epidermis cells with thin walls, similar to those found in Moreno-Terrazas et al. [74]. Also, there were mineralized structures with calcium crystals as detected by EDX (Fig. 7). These structures could be cell walls, which usually contain calcium [75]. Unlike the chestnut shell, in which no relevant differences were observed when using classical or flash pyrolysis, in the case of the grape seed it can be observed that flash

pyrolysis causes explosive-type hollows in the carbonaceous matter (Fig. 6c), probably due to the rapid release of the volatile matter [23].

4. Conclusions

This work encompassed the conventional and flash pyrolytic energetic valorisation of grape seeds (GS) and chestnut shell (CH) residues. Their thermogravimetric analysis made it possible to choose the ideal experimental parameters. DTG$_{max}$ values were higher for CH possibly due to its higher hemicellulose and cellulose content. Kinetic parameters rated E$_a$ values 212.35–217.19 kJ mol^{-1} for CH and 336.83–349.13 kJ mol^{-1} for GS. Slower heating rates minimized the thermal cracking reactions taking place within the biomass, resulting in higher yields of biochar (37.6% *vs.* 33.2% for GS and 29.2% *vs.* 26.6% for CH). Biochar obtained for both samples was suitable as a fuel (HHV in the range 26.6–32.7 MJ kg^{-1}) and as activated carbon precursors (77.5–91.5% of carbon content and 2.4–10.2% of ash content). Flash pyrolysis (PF) favoured the production of gaseous fraction in both residues (~15% higher for GS and ~5% for CH). HHV results of gases derived from PF quadrupled those from conventional pyrolysis (PC) due to the increase in fuel gases (H$_2$, CH$_4$, C$_2$H$_4$) and their lower CO$_2$ content. The bio-oil yield in both residues was always higher in PC. Bio-oil composition of those obtained from PF and PC presented differences with up to 90% of PAH in PF derived bio-oil. According to these results, pyrolysis techniques can be appropriate for the valorisation of these residues. Depending on the specific fraction to be obtained, it will be necessary to opt for certain pyrolytic conditions in accordance with the results here depicted.

Data availability

Data will be made available on request.

Appendix A. Supplementary data

Supplementary data to this article can be found online at https://doi.org/10.1016/j.biombioe.2023.106942.

References

[1] B. Tian, J. Wang, Y. Qiao, H. Huang, L. Xu, Y. Tian, Understanding the pyrolysis synergy of biomass and coal blends based on volatile release, kinetics and char structure, Biomass Bioenergy 168 (2023), 106687, https://doi.org/10.1016/J.BIOMBIOE.2022.106687.

[2] F. Xu, S.I. Okopi, Y. Jiang, Z. Chen, L. Meng, Y. Li, W. Sun, C. Li, Multi-criteria assessment of food waste and waste paper anaerobic co-digestion: effects of inoculation ratio, total solids content, and feedstock composition, Renew. Energy 194 (2022) 40–50, https://doi.org/10.1016/J.RENENE.2022.05.078.

[3] S. Kant Bhatia, A.K. Palai, A. Kumar, R. Kant Bhatia, A. Kumar Patel, V. Kumar Thakur, Y.H. Yang, Trends in renewable energy production employing biomass-based biochar, Bioresour. Technol. 340 (2021), 125644, https://doi.org/10.1016/J.BIORTECH.2021.125644.

[4] G. San Miguel, F. Sánchez, A. Pérez, L. Velasco, One-step torrefaction and densification of woody and herbaceous biomass feedstocks, Renew. Energy 195 (2022) 825–840, https://doi.org/10.1016/J.RENENE.2022.06.085.

[5] T. Kober, H.W. Schiffer, M. Densing, E. Panos, Global energy perspectives to 2060 – WEC's world energy scenarios 2019, Energy Strategy Rev. 31 (2020), 100523, https://doi.org/10.1016/J.ESR.2020.100523.

[6] R.K. Mishra, K. Mohanty, Kinetic analysis and pyrolysis behaviour of waste biomass towards its bioenergy potential, Bioresour. Technol. 311 (2020), 123480, https://doi.org/10.1016/J.BIORTECH.2020.123480.

[7] T.Y.A. Fahmy, Y. Fahmy, F. Mobarak, M. El-Sakhawy, R.E. Abou-Zeid, Biomass pyrolysis: past, present, and future, Environment, Development and Sustainability 2018 22:1 22 (2018) 17–32, https://doi.org/10.1007/S10668-018-0200-5.

[8] S.Y. Huang, C.Y. Chen, W.Y. Hsu, A.N. Huang, H.P. Kuo, Simulation of biomass pyrolysis in a fluidized bed reactor: independent sand, biomass and char granular phases, Biomass Bioenergy 173 (2023), 106796, https://doi.org/10.1016/J.BIOMBIOE.2023.106796.

[9] Z. Chu, Y. Li, C. Zhang, Y. Fang, J. Zhao, A review on resource utilization of oil sludge based on pyrolysis and gasification, J. Environ. Chem. Eng. 11 (2023), 109692, https://doi.org/10.1016/J.JECE.2023.109692.

[10] J. Proano-Aviles, J.K. Lindstrom, P.A. Johnston, R.C. Brown, Heat and mass transfer effects in a furnace-based micropyrolyzer, Energy Technol. 5 (2017) 189–195, https://doi.org/10.1002/ENTE.201600279.

[11] J.O. Ighalo, F.U. Iwuchukwu, O.E. Eyankware, K.O. Iwuozor, K. Olotu, O.C. Bright, C.A. Igwegbe, Flash pyrolysis of biomass: a review of recent advances, Clean Technol. Environ. Policy 24 (2022) 2349–2363, https://doi.org/10.1007/S10098-022-02339-5/TABLES/6.

[12] A.M. Elgarahy, A. Hammad, D.M. El-Sherif, M. Abouzid, M.S. Gaballah, K.Z. Elwakeel, Thermochemical conversion strategies of biomass to biofuels, techno-economic and bibliometric analysis: a conceptual review, J. Environ. Chem. Eng. 9 (2021), 106503, https://doi.org/10.1016/J.JECE.2021.106503.

[13] M. Sekar, T. Mathimani, A. Alagumalai, N.T.L. Chi, P.A. Duc, S.K. Bhatia, K. Brindhadevi, A. Pugazhendhi, A review on the pyrolysis of algal biomass for biochar and bio-oil – bottlenecks and scope, Fuel 283 (2021), 119190, https://doi.org/10.1016/J.FUEL.2020.119190.

[14] A. Bieniek, M. Reinmöller, F. Küster, M. Gräbner, W. Jerzak, A. Magdziarz, Investigation and modelling of the pyrolysis kinetics of industrial biomass wastes, J. Environ. Manag. 319 (2022), 115707, https://doi.org/10.1016/J.JENVMAN.2022.115707.

[15] J.E.B. Costa, A.S. Barbosa, M.A.F. Melo, D.M.A. Melo, R.L.B.A. Medeiros, R.M. Braga, Renewable aromatics through catalytic pyrolysis of coconut fiber (Cocos nucífera Linn.) using low cost HZSM-5, Renew. Energy 191 (2022) 439–446, https://doi.org/10.1016/J.RENENE.2022.03.111.

[16] Y. Li, Y. Wang, M. Chai, C. Li, Nishu, D. Yellezuome, R. Liu, Pyrolysis kinetics and thermodynamic parameters of bamboo residues and its three main components using thermogravimetric analysis, Biomass Bioenergy 170 (2023), 106705, https://doi.org/10.1016/J.BIOMBIOE.2023.106705.

[17] T. Somorin, L.C. Campos, J.R. Kinobe, R.N. Kulabako, O.O.D. Afolabi, Sustainable valorisation of agri-food waste from open-air markets in Kampala, Uganda via standalone and integrated waste conversion technologies, Biomass Bioenergy 172 (2023), 106752, https://doi.org/10.1016/J.BIOMBIOE.2023.106752.

[18] Y.K.S.S. Rao, C.S. Dhanalakshmi, D.K. Vairavel, R. Surakasi, S. Kaliappan, P.P. Patil, S. Socrates, J.I.J. Lalvani, Investigation on forestry wood wastes: pyrolysis and thermal characteristics of Ficus religiosa for energy recovery system, Adv. Mater. Sci. Eng. 2022 (2022), https://doi.org/10.1155/2022/3314606.

[19] K. Filippi, H. Papapostolou, M. Alexandri, A. Vlysidis, E.D. Myrtsi, D. Ladakis, C. Pateraki, S.A. Haroutounian, A. Koutinas, Integrated biorefinery development using winery waste streams for the production of bacterial cellulose, succinic acid and value-added fractions, Bioresour. Technol. (2021), 125989, https://doi.org/10.1016/J.BIORTECH.2021.125989.

[20] Y. Ding, S. Yu, J. Wang, M. Li, C. Qu, J. Li, L. Liu, Comparative transcriptomic analysis of seed coats with high and low lignin contents reveals lignin and flavonoid biosynthesis in Brassica napus, BMC Plant Biol. 21 (2021) 1–16, https://doi.org/10.1186/S12870-021-03030-5/FIGURES/9.

[21] M. Munir, M. Ahmad, A. Waseem, M. Zafar, M. Saeed, A. Wakeel, M. Nazish, S. Sultana, Scanning electron microscopy leads to identification of novel nonedible oil seeds as energy crops, Microsc. Res. Tech. 82 (2019) 1165–1173, https://doi.org/10.1002/JEMT.23265.

[22] V.O. Santos, L.S. Queiroz, R.O. Araujo, F.C.P. Ribeiro, M.N. Guimarães, C.E.F. da Costa, J.S. Chaar, L.K.C. de Souza, Pyrolysis of acai seed biomass: kinetics and thermodynamic parameters using thermogravimetric analysis, Bioresour. Technol. Rep. 12 (2020), 100553, https://doi.org/10.1016/J.BITEB.2020.100553.

[23] D. Jimenez-Cordero, F. Heras, N. Alonso-Morales, M.A. Gilarranz, J.J. Rodriguez, Porous structure and morphology of granular chars from flash and conventional pyrolysis of grape seeds, Biomass Bioenergy 54 (2013) 123–132, https://doi.org/10.1016/J.BIOMBIOE.2013.03.020.

[24] F. Bianco, H. Şenol, S. Papirio, Enhanced lignocellulosic component removal and biomethane potential from chestnut shell by a combined hydrothermal–alkaline pretreatment, Sci. Total Environ. 762 (2021), 144178, https://doi.org/10.1016/J.SCITOTENV.2020.144178.

[25] S. Rodríguez-Sánchez, B. Ruiz, D. Martínez-Blanco, M. Sánchez-Arenillas, M.A. Diez, I. Suárez-Ruiz, J.F. Marco, J. Blanco, E. Fuente, Sustainable thermochemical single-step process to obtain magnetic activated carbons from chestnut industrial wastes, ACS Sustain. Chem. Eng. 7 (2019) 17293–17305, https://doi.org/10.1021/ACSSUSCHEMENG.9B04141.

[26] T. Rasool, I. Najar, V.C. Srivastava, A. Pandey, Pyrolysis of almond (Prunus amygdalus) shells: kinetic analysis, modelling, energy assessment and technical feasibility studies, Bioresour. Technol. 337 (2021), 125466, https://doi.org/10.1016/J.BIORTECH.2021.125466.

[27] M. del C. Rojas, M.L. Nieva Lobos, M.L. Para, M.E. González Quijón, O. Cámara, D. Barraco, E.L. Moyano, G.L. Luque, Activated carbon from pyrolysis of peanut shells as cathode for lithium-sulfur batteries, Biomass Bioenergy 146 (2021), 105971, https://doi.org/10.1016/J.BIOMBIOE.2021.105971.

[28] B. Ruiz, E. Ruisánchez, R.R. Gil, N. Ferrera-Lorenzo, M.S. Lozano, E. Fuente, Sustainable porous carbons from lignocellulosic wastes obtained from the extraction of tannins, Microporous Mesoporous Mater. 209 (2015) 23–29, https://doi.org/10.1016/J.MICROMESO.2014.09.004.

[29] P.L. Dulong, A.T. Petit, Recherches sur la mesure des temperatures et sur les lois de la communication de la chaleur, first ed., De l'Imprimerie Royale, 1818.

[30] D. Beckman, Techno-economic Assessment of Selected Biomass Liquefaction Processes, Valtion Teknillinen Tutkimuskeskus, 1990.

[31] S. Paniagua, S. Reyes, F. Lima, N. Pilipenko, L.F. Calvo, Combustion of avocado crop residues: effect of crop variety and nature of nutrients, Fuel 291 (2021), 119660, https://doi.org/10.1016/J.FUEL.2020.119660.

[32] R.K. Mishra, K. Mohanty, X. Wang, Pyrolysis kinetic behavior and Py-GC–MS analysis of waste dahlia flowers into renewable fuel and value-added chemicals, Fuel 260 (2020), 116338, https://doi.org/10.1016/J.FUEL.2019.116338.

[33] A. Pérez, B. Ruiz, E. Fuente, L.F. Calvo, S. Paniagua, Pyrolysis technology for Cortaderia selloana invasive species. Prospects in the biomass energy sector, Renew. Energy 169 (2021) 178–190, https://doi.org/10.1016/J.RENENE.2021.01.015.

[34] W. Saadi, S. Rodríguez-Sánchez, B. Ruiz, S. Souissi-Najar, A. Ouederni, E. Fuente, Pyrolysis technologies for pomegranate (Punica granatum L.) peel wastes. Prospects in the bioenergy sector, Renew. Energy 136 (2019) 373–382, https://doi.org/10.1016/J.RENENE.2019.01.017.

[35] B. Ruiz, E. Fuente, A. Pérez, L. Taboada-Ruiz, J.M. Sanz, L.F. Calvo, S. Paniagua, Employment of conventional and flash pyrolysis for biomass wastes from the textile industry with sustainable prospects, J. Anal. Appl. Pyrolysis 169 (2023), 105864, https://doi.org/10.1016/J.JAAP.2023.105864.

[36] K. Yang, J. Huang, B. Dong, P. Liu, L. Chen, Z. Wang, L. Jia, Secondary reactions of primary tar from biomass pyrolysis: characterization of heavy products by FT-ICR MS, Energy Fuel. 35 (2021) 13191–13199, https://doi.org/10.1021/ACS.ENERGYFUELS.1C01723/SUPPL_FILE/EF1C01723_SI_001.PDF.

[37] O. Sanahuja-Parejo, A. Veses, M.V. Navarro, J.M. López, R. Murillo, M.S. Callén, T. García, Catalytic co-pyrolysis of grape seeds and waste tyres for the production of drop-in biofuels, Energy Convers. Manag. 171 (2018) 1202–1212, https://doi.org/10.1016/J.ENCONMAN.2018.06.053.

[38] V. Dhyani, T. Bhaskar, A comprehensive review on the pyrolysis of lignocellulosic biomass, Renew. Energy 129 (2018) 695–716, https://doi.org/10.1016/J.RENENE.2017.04.035.

[39] S.v. Vassilev, C.G. Vassileva, Y.C. Song, W.Y. Li, J. Feng, Ash contents and ash-forming elements of biomass and their significance for solid biofuel combustion, Fuel 208 (2017) 377–409, https://doi.org/10.1016/J.FUEL.2017.07.036.

[40] C. Marculescu, S. Ciuta, Wine industry waste thermal processing for derived fuel properties improvement, Renew. Energy 57 (2013) 645–652, https://doi.org/10.1016/J.RENENE.2013.02.028.

[41] G. Özsin, A.E. Pütün, Kinetics and evolved gas analysis for pyrolysis of food processing wastes using TGA/MS/FT-IR, Waste Manag. 64 (2017) 315–326, https://doi.org/10.1016/J.WASMAN.2017.03.020.

[42] L.P. Cruz-Lopes, I. Domingos, J. Ferreira, B. Esteves, Chemical composition and study on liquefaction optimization of chestnut shells, Open Agric 5 (2020) 905–911, https://doi.org/10.1515/OPAG-2020-0089/MACHINEREADABLECITATION/RIS.

[43] P. McKendry, Energy production from biomass (part 1): overview of biomass, Bioresour. Technol. 83 (2002) 37–46, https://doi.org/10.1016/S0960-8524(01)00118-3.

[44] E. Butnaru, D. Pamfil, E. Stoleru, M. Brebu, Characterization of bark, needles and cones from silver fir (Abies alba mill.) towards valorization of biomass forestry residues, Biomass Bioenergy 159 (2022), 106413, https://doi.org/10.1016/J.BIOMBIOE.2022.106413.

[45] E. Espinosa, E. Rincón, R. Morcillo-Martín, L. Rabasco-Vílchez, A. Rodríguez, Orange peel waste biorefinery in multi-component cascade approach: polyphenolic

compounds and nanocellulose for food packaging, Ind. Crops Prod. 187 (2022), 115413, https://doi.org/10.1016/J.INDCROP.2022.115413.

[46] L. Cruz-lopes, Y. Dulyanska, I. Domingos, J. Ferreira, A. Fragata, R. Guiné, B. Esteves, Influence of pre-hydrolysis on the chemical composition of prunus avium cherry seeds, Agronomy 2022 12 (2022) 280, https://doi.org/10.3390/AGRONOMY12020280, 280. 12.

[47] T. Uysal, G. Duman, Y. Onal, I. Yasa, J. Yanik, Production of activated carbon and fungicidal oil from peach stone by two-stage process, J. Anal. Appl. Pyrolysis 108 (2014) 47–55, https://doi.org/10.1016/J.JAAP.2014.05.017.

[48] M.P. Elizalde-González, V. Hernández-Montoya, Characterization of mango pit as raw material in the preparation of activated carbon for wastewater treatment, Biochem. Eng. J. 36 (2007) 230–238, https://doi.org/10.1016/J.BEJ.2007.02.025.

[49] S. Paniagua Bermejo, A. Prado-Guerra, A.I. García Pérez, L.F. Calvo Prieto, Study of quinoa plant residues as a way to produce energy through thermogravimetric analysis and indexes estimation, Renew. Energy 146 (2020) 2224–2233, https://doi.org/10.1016/J.RENENE.2019.08.056.

[50] M. Garca-Pèrez, A. Chaala, J. Yang, C. Roy, Co-pyrolysis of sugarcane bagasse with petroleum residue. Part I: thermogravimetric analysis, Fuel 80 (2001) 1245–1258, https://doi.org/10.1016/S0016-2361(00)00215-5.

[51] V. Hernández-Montoya, M.A. Montes-Morán, M.P. Elizalde-González, Study of the thermal degradation of citrus seeds, Biomass Bioenergy 33 (2009) 1295–1299, https://doi.org/10.1016/J.BIOMBIOE.2009.05.016.

[52] S. Paniagua, L. Zanfaño, L.F. Calvo, Influence of the fertilizer type in the agronomic and energetic behaviour of the residues coming from oleander, cypress and quinoa, Fuel 272 (2020), 117711, https://doi.org/10.1016/J.FUEL.2020.117711.

[53] Z. Chen, Q. Zhu, X. Wang, B. Xiao, S. Liu, Pyrolysis behaviors and kinetic studies on Eucalyptus residues using thermogravimetric analysis, Energy Convers. Manag. 105 (2015) 251–259, https://doi.org/10.1016/J.ENCONMAN.2015.07.077.

[54] S.L. Narnaware, N.L. Panwar, Kinetic study on pyrolysis of mustard stalk using thermogravimetric analysis, Bioresour. Technol. Rep. 17 (2022), 100942, https://doi.org/10.1016/J.BITEB.2021.100942.

[55] T. Shen, F. Zhang, S. Yang, Y. Wang, H. Liu, H. Wang, J. Hu, Comprehensive study on the pyrolysis process of chestnut processing waste (chestnut shells): kinetic triplet, thermodynamic, in-situ monitoring of evolved gasses and analysis biochar, Fuel 331 (2023) 125944, https://doi.org/10.1016/J.FUEL.2022.125944.

[56] A.N. Amenaghawon, C.L. Anyalewechi, C.O. Okieimen, H.S. Kusuma, Biomass pyrolysis technologies for value-added products: a state-of-the-art review, Environment, Development and Sustainability 2021 23:10 23 (2021) 14324–14378, https://doi.org/10.1007/S10668-021-01276-5.

[57] C. Tsekos, K. Anastasakis, P.L. Schoenmakers, W. de Jong, PAH sampling and quantification from woody biomass fast pyrolysis in a pyroprobe reactor with a modified tar sampling system, J. Anal. Appl. Pyrolysis 147 (2020), 104802, https://doi.org/10.1016/J.JAAP.2020.104802.

[58] R. Kumar, V. Strezov, H. Weldekidan, J. He, S. Singh, T. Kan, B. Dastjerdi, Lignocellulose biomass pyrolysis for bio-oil production: a review of biomass pre-treatment methods for production of drop-in fuels, Renew. Sustain. Energy Rev. 123 (2020), 109763, https://doi.org/10.1016/J.RSER.2020.109763.

[59] K. Alper, K. Tekin, S. Karagöz, Pyrolysis of agricultural residues for bio-oil production, Clean Technol. Environ. Policy 17 (2015) 211–223, https://doi.org/10.1007/S10098-014-0778-8/FIGURES/9.

[60] B. Ruiz, N. Ferrera-Lorenzo, E. Fuente, Valorisation of lignocellulosic wastes from the candied chestnut industry. Sustainable activated carbons for environmental applications, J. Environ. Chem. Eng. 5 (2017) 1504–1515, https://doi.org/10.1016/J.JECE.2017.02.028.

[61] T. Kan, V. Strezov, T.J. Evans, Lignocellulosic biomass pyrolysis: a review of product properties and effects of pyrolysis parameters, Renew. Sustain. Energy Rev. 57 (2016) 1126–1140, https://doi.org/10.1016/J.RSER.2015.12.185.

[62] Y. Chai, N. Gao, M. Wang, C. Wu, H2 production from co-pyrolysis/gasification of waste plastics and biomass under novel catalyst Ni-CaO-C, Chem. Eng. J. 382 (2020), 122947, https://doi.org/10.1016/J.CEJ.2019.122947.

[63] T. Matamba, A. Tahmasebi, S. Khoshk Rish, J. Yu, Promotion Effects of Pressure on Polycyclic Aromatic Hydrocarbons and H2 Formation during Flash Pyrolysis of Palm Kernel Shell, Energy and Fuels, 2020, https://doi.org/10.1021/ACS.ENERGYFUELS.9B04409/SUPPL_FILE/EF9B04409_SI_001.PDF.

[64] M.Y. Khan, Z.A. Abdul Karim, A.R.A. Aziz, I.M. Tan, Performance and emission assessment of multi cylinder diesel engine using surfactant enhanced water in diesel emulsion, MATEC Web of Conferences 13 (2014), 02025, https://doi.org/10.1051/MATECCONF/20141302025.

[65] J. Deng, X. Wang, Z. Wei, L. Wang, C. Wang, Z. Chen, A review of NOx and SOx emission reduction technologies for marine diesel engines and the potential evaluation of liquefied natural gas fuelled vessels, Sci. Total Environ. 766 (2021), 144319, https://doi.org/10.1016/J.SCITOTENV.2020.144319.

[66] W. Gerbens-Leenes, A.Y. Hoekstra, T.H. van der Meer, The water footprint of bioenergy, Proc. Natl. Acad. Sci. U. S. A. 106 (2009) 10219–10223, https://doi.org/10.1073/PNAS.0812619106/SUPPL_FILE/0812619106SI.PDF.

[67] K. Wiedner, C. Rumpel, C. Steiner, A. Pozzi, R. Maas, B. Glaser, Chemical evaluation of chars produced by thermochemical conversion (gasification, pyrolysis and hydrothermal carbonization) of agro-industrial biomass on a commercial scale, Biomass Bioenergy 59 (2013) 264–278, https://doi.org/10.1016/J.BIOMBIOE.2013.08.026.

[68] J. Yu, K. Maliutina, A. Tahmasebi, A review on the production of nitrogen-containing compounds from microalgal biomass via pyrolysis, Bioresour. Technol. 270 (2018) 689–701, https://doi.org/10.1016/J.BIORTECH.2018.08.127.

[69] S. Rodríguez-Sánchez, B. Ruiz, D. Martínez-Blanco, M. Sánchez-Arenillas, M. A. Diez, J.F. Marco, P. Gorria, E. Fuente, Towards advanced industrial waste-based magnetic activated carbons with tunable chemical, textural and magnetic properties, Appl. Surf. Sci. 551 (2021), 149407, https://doi.org/10.1016/J.APSUSC.2021.149407.

[70] A. Anand, S. Gautam, L.C. Ram, Feedstock and pyrolysis conditions affect suitability of biochar for various sustainable energy and environmental applications, J. Anal. Appl. Pyrolysis 170 (2023), 105881, https://doi.org/10.1016/J.JAAP.2023.105881.

[71] C. Primaz, O. Gil-Castell, A. Ribes-Greus, Strategies towards thermochemical valorisation of spent coffee grounds (SCG): kinetic analysis of the thermal and thermo-oxidative decomposition, Biomass Bioenergy 174 (2023), 106840, https://doi.org/10.1016/J.BIOMBIOE.2023.106840.

[72] A. Bazargan, S.L. Rough, G. McKay, Compaction of palm kernel shell biochars for application as solid fuel, Biomass Bioenergy 70 (2014) 489–497, https://doi.org/10.1016/J.BIOMBIOE.2014.08.015.

[73] J.C. Ang, J.Y. Tang, B.Y.H. Chung, J.W. Chong, R.R. Tan, K.B. Aviso, N. G. Chemmangattuvalappil, S. Thangalazhy-Gopakumar, Development of predictive model for biochar surface properties based on biomass attributes and pyrolysis conditions using rough set machine learning, Biomass Bioenergy 174 (2023), 106820, https://doi.org/10.1016/J.BIOMBIOE.2023.106820.

[74] R. Moreno-Terrazas, F.J. Flores-Tena, M.D. Barba-Avila, A.L. Guerrero-Barrera, F. J. Avelar-Gonzalez, E.M. Ramirez-Lopez, A comparative analysis of microflora during biofilm development on grape seeds exposed to methanol in a biofilter, World J. Microbiol. Biotechnol. 26 (2010) 657–664, https://doi.org/10.1007/S11274-009-0219-8/FIGURES/4.

[75] P. Bauer, R. Elbaum, I.M. Weiss, Calcium and silicon mineralization in land plants: transport, structure and function, Plant Sci. 180 (2011) 746–756, https://doi.org/10.1016/J.PLANTSCI.2011.01.019.